Parallax Errors and Corrections for Dual-Antenna Millimeter-Wave Cloud Radars

STEPHEN M. SEKELSKY

Microwave Remote Sensing Laboratory, University of Massachusetts—Amherst, Amherst, Massachusetts

EUGENE E. CLOTHIAUX

The Pennsylvania State University, University Park, Pennsylvania

(Manuscript received 13 April 2001, in final form 4 October 2001)

ABSTRACT

Dual-antenna radar designs avoid using a transmit/receive switch. In order to measure radar reflectivity accurately and to avoid a general decrease in system sensitivity, these systems require precise alignment of their high-gain/narrow-beamwidth antennas, which is difficult. Given precisely aligned antennas, a parallax correction to account for antenna beam overlap, which is range-dependent, must be used with the correct alignment information to produce accurate reflectivities. Calculations show that dual-antenna parallax errors are extremely sensitive to the alignment of the two antennas, especially for the current generation of W-band radars, which tend to use 0.91- and 1.21-m Cassegrain antennas with half-power beamwidths of typically $\leq 0.25°$. For example, the minimum detectable reflectivity of a W-band radar system may be degraded by more than an order of magnitude for alignment errors on the order of the antenna half-power beamwidth. Moreover, parallax errors are essentially independent of range at cirrus altitudes, and it is not possible to separate parallax effects from offsets in calibration at these far ranges. Observations from a field experiment that include both single- and dual-antenna radar measurements are used to demonstrate these points. Alignment problems have led to the abandonment of dual-antenna pulsed W-band systems in the cloud remote sensing community, and the current generation of millimeter-wave frequency-modulated continuous wave systems must properly take these problems into consideration.

1. Introduction

Early pulsed millimeter-wave (MMW) radar systems (Hobbs et al. 1985; Lhermitte 1987; Mead et al. 1991) and current designs for frequency-modulated continuous wave (FMCW) MMW systems (Klugmann and Judaschke 1995) use separate transmit and receive antennas as a cost effective means to isolate the receiver from the transmitter. These dual antenna radars require a range-dependent beam overlap, or parallax, correction to accurately determine the radar cross section of a target. Parallax is significant at short distances, where the beams have little overlap, but decreases to unity with increasing range. Given the shape of the antenna patterns, this correction is calculated in a straightforward manner when the antenna bore sights, or directions of peak gain, are aligned parallel to one another. Difficulties occur, however, when high-gain, narrow-beam antennas are used, because the parallax correction is quite sensitive to the relative alignment of the two antennas.

Alignment tolerances can be relaxed for terrestrial or ocean surface sensing systems by using low-gain broad-beam antennas because signal-to-noise ratios are large. Unfortunately, cloud echoes are sufficiently weak that gain cannot be sacrificed for MMW systems used in cloud remote sensing studies. Dual-antenna atmospheric radars typically employ two identical high-gain/narrow-beam antennas aligned by maximizing the echo from a distant target, such as a cirrus cloud. At W-band (95 GHz) frequencies antenna diameters are on the order of 1 m, with a half-power beamwidth (θ_o) of approximately 0.25° or smaller.

To illustrate the relevance of dual-antenna pointing errors, we first present the radar equation for atmospheric targets that includes a parallax correction factor [$f(r)$] to account for the range (r) dependent antenna beam overlap for the two antennas. [Note that $f(r)$ is unity at all ranges r for a single-antenna radar.] A simple model for the parallax correction factor [$f(r)$] is subsequently developed and used to assess sensitivity to antenna misalignment and transmit pulse length. Since pulse-length effects are minimal outside of the antenna near field, a simplified version of the parallax model that is independent of pulse length is developed.

The simplified parallax model is subsequently applied to observations from the dual-antenna Pennsylvania

Corresponding author address: Dr. Stephen M. Sekelsky, Microwave Remote Sensing Laboratory, University of Massachusetts—Amherst, Knowles 209C, Amherst, MA 01003.
E-mail: sekelsky@mirsl.ecs.umass.edu

State University (Penn State) radar system (Clothiaux et al. 1995) using collocated measurements from the University of Massachusetts (UMass) single-antenna Cloud Profiling Radar System (CPRS; Sekelsky and McIntosh 1996) as a reference. (System parameters for these radars are listed in Table 1). Because $f(r)$ is unity for a single-antenna system, $f(r)$ for the dual antenna radar can be obtained as the ratio of the dual-antenna to single-antenna radar reflectivity, apart from a constant that accounts for system calibration differences. A comparison of vertically pointing observations from low-altitude liquid clouds and high-altitude cirrus clouds is used to determine the Penn State radar system parallax correction, antenna misalignment, and calibration offset with respect to the UMass radar system. The consequences of imperfect antenna alignment are subsequently discussed in the context of quantifying the absolute radar calibration.

2. Methodology

a. Radar equation with a parallax correction factor

The radar equation for meteorological targets is described in various texts and articles, including Doviak and Zrnić (1984), Smith (1986), and Battan (1973). For the discussion here we note that the received power reflected from clouds or precipitation is proportional to the size of the radar sample volume (V):

$$\overline{P}_r = \beta \frac{VZ_e}{r^4}, \tag{1}$$

where $\overline{P}_r$ is the average received power referenced to the digitizer input, V is the radar sample volume, Z_e is the equivalent radar reflectivity factor, β is a constant, and r is the range to the center of the sampling volume. For a single-antenna radar with a Gaussian beam the volume (V) can be approximated as a simple function of antenna half-power antenna beamwidth (θ_o) and pulse length (τ), as described in Doviak and Zrnić (1984).

For a dual-antenna radar, Eq. (1) is multiplied with a parallax correction factor [$f(r)$], which is a complex function of radar geometry and transmit and receive antenna characteristics, and the radar equation becomes

$$P_r = \beta \frac{VZ_e}{r^4} f(r). \tag{2}$$

In Eq. (2), V is the sample volume of one antenna, while $f(r)$ accounts for the range-dependent overlap of the transmit and receive antenna beams.

b. Numerical model of dual-antenna parallax

The sample volume for a single-antenna pulsed radar with a Gaussian beam is given by

$$V_{\text{single}}(z) = \int_{z-c\tau/4}^{z+c\tau/4} \int_{y=-\infty}^{+\infty} \int_{x=-\infty}^{+\infty} \left(\exp\left\{ -\left[\frac{x}{\sigma_x(z')} \right]^2 \right\} \exp\left\{ -\left[\frac{y}{\sigma_y(z')} \right]^2 \right\} \right)^2 dx\, dy\, dz'. \tag{3}$$

In Eq. (3) the antenna points in the z direction, which coincides with the range dimension (r), and only the main beam is considered since side lobe contributions are negligible for most MMW cloud radar systems. The parameters $\sigma_x(z)$ and $\sigma_y(z)$ are obtained from the antenna half-power beamwidth (θ_o). Ferraro (1992) shows that, for a Gaussian antenna pattern,

$$\sigma(z) = \frac{z\theta_o}{1.665}. \tag{4}$$

Because antenna beamwidth may not be identical in the xz and yz planes, $\sigma_x(z)$ and $\sigma_y(z)$ are explicit in Eq. (3).

The sample volume for a two-antenna radar is derived for the configuration shown in Fig. 1, where the beam for one antenna (No. 1) is fixed pointing in the z direction, and the beam direction for the second antenna (No. 2) varies to simulate alignment error. The angles θ_s and ϕ_s quantify alignment errors, or offsets, from the z direction in the yz and xz planes, respectively. The distance Δ represents the physical separation of the two antennas, which lie along the y axis. Using this geometry, we model the sample volume for a dual-antenna radar as the overlap between the transmit and receive antenna beams:

$$V_{\text{dual}}(z) \approx \int_{z-c\tau/4}^{z+c\tau/4} \int_{y=-\infty}^{+\infty} \int_{x=-\infty}^{+\infty} \left(\exp\left\{ -\left[\frac{x}{\sigma_x(z')} \right]^2 \right\} \exp\left\{ -\left[\frac{y}{\sigma_y(z')} \right]^2 \right\} \right) \times \left(\exp\left\{ -\left[\frac{x + z' \sin(\phi_s)}{\sigma_x(z')} \right]^2 \right\} \exp\left\{ -\left[\frac{y + z' \sin(\theta_s) + \Delta}{\sigma_y(z')} \right]^2 \right\} \right) dx\, dy\, dz'. \tag{5}$$

TABLE 1. UMass and Penn State radar parameters.

	CPRS (33 GHz)	CPRS (95 GHz)	Penn State (94 GHz)
Frequency (GHz)	33.12	94.92	93.95
Peak power (kW)	120	1.5	1.4
Average power (W)	120	15	15
Pulse repetion frequency (Hz)	200–3000	1–20 000	1–20 000
Pulse width (ns)	200–2000	50–2000	50–2000
Noise figure (dB)	11	13	8.1
3-dB bandwidth (MHz)	2	18	58
Antenna	1-m lens	1-m lens	two 0.91-m Cassegrains
3-dB beamwidth (deg)	0.601	0.208	0.22
Min detectable Z (dBZ) (1-s averaging time, $\tau = 500$ ns, $r = 1$ km)	−56.8	−46.9	−47.0

The parallax correction factor [$f(r)$] in Eq. (2) is defined as the ratio of the dual-antenna radar sample volume to that for the single-antenna radar:

$$f(r) = \frac{V_{\text{dual}}(r)}{V_{\text{single}}(r)}, \tag{6}$$

where z is replaced by r in Eqs. (3) and (4).

Note that Eq. (6) can be simplified by eliminating dependence on pulse length (τ), because $f(r)$ is only sensitive to τ at short distances. This property of $f(r)$ is illustrated in Fig. 2, which shows $f(r)$ for $\Delta = 1$ m and $\theta_o = 0.2°$ using several pulse lengths. Beyond a few hundred meters the different curves are indistinguishable from one another. Because single-antenna MMW cloud radars have transmit/receive switches with finite switching speeds that limit their minimum distance to a few hundred meters, eliminating τ from Eq. (6) has little impact on the present set of comparisons. We therefore approximate $f(r)$ as

$$f(r) \approx \frac{V'_{\text{dual}}(r)}{V'_{\text{single}}(r)}, \tag{7}$$

where

$$V'_{\text{single}}(r) = \frac{c\tau}{2} \int_{y=-\infty}^{+\infty} \int_{x=-\infty}^{+\infty} \left(\exp\left\{ -\left[\frac{x}{\sigma_x(r)} \right]^2 \right\} \exp\left\{ -\left[\frac{y}{\sigma_y(r)} \right]^2 \right\} \right)^2 dx\, dy \quad \text{and} \tag{8}$$

$$V'_{\text{dual}}(r) = \frac{c\tau}{2} \int_{y=-\infty}^{+\infty} \int_{x=-\infty}^{+\infty} \left(\exp\left\{ -\left[\frac{x}{\sigma_x(r)} \right]^2 \right\} \exp\left\{ -\left[\frac{y}{\sigma_y(r)} \right]^2 \right\} \right) \times \left(\exp\left\{ -\left[\frac{x + r \sin(\sigma_s)}{\sigma_x(r)} \right]^2 \right\} \exp\left\{ -\left[\frac{y + r \sin(\theta_s) + \Delta}{\sigma_y(r)} \right]^2 \right\} \right) dx\, dy. \tag{9}$$

When Eqs. (8) and (9) are substituted into Eq. (7), $c\tau/2$ is found in both the numerator and denominator, thus eliminating dependence on pulse length. Equation (7) is represented by the solid line in Fig. 2.

Application of Eq. (7) to the Penn State radar system yields the results in Figs. 3 and 4. As Fig. 3 shows, $f(r)$ is symmetric versus ϕ_s and drops off rapidly as the absolute value of ϕ_s increases. The factor $f(r)$ is equally sensitive to θ_s, but the dependence of $f(r)$ on θ_s is not symmetric, as the two families of curves for positive and negative values of θ_s illustrate in Fig. 4. (Note that, in Fig. 4, $\phi_s = 0$ and the dotted curves represent the baseline correction that is used when the antenna beams are aligned parallel to one another.) In practice, the beams are aligned by maximizing the echo from a distant target, such as a cirrus cloud, and applying the baseline curve. It is normally assumed that the two antenna beams are exactly parallel with $\theta_s = 0$ and $\phi_s = 0$. However, Fig. 4 makes clear that $f(r)$ is extremely sensitive to alignment errors of the 0.2° beamwidth antennas used on the Penn State radar.

Antenna misalignment leads to reflectivity errors and to a general reduction in system sensitivity. At near range the reflectivity error can be larger or smaller than the baseline correction depending upon the sign of θ_s. At far range misalignment leads to underestimation of radar reflectivity. These calculations indicate that angular errors on the order of the half-power beamwidth (θ_o) translate into reflectivity errors and sensitivity reductions on the order of 10 dB. For angular errors of twice the half-power beamwidth, sensitivity is reduced by approximately 50 dB.

The dependence of the baseline $f(r)$ on antenna separation (Δ) is presented in Fig. 5 for several altitudes.

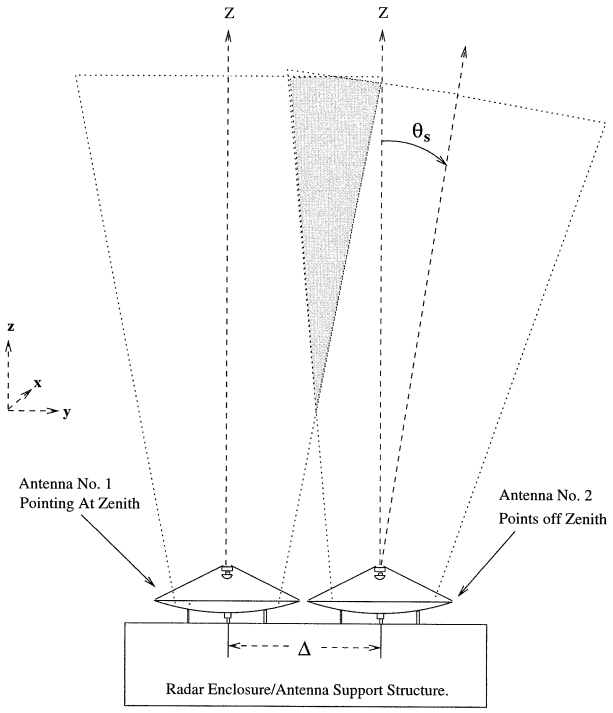

Beam overlap for dual antenna system with non-parallel beams

FIG. 1. Geometry for two-antenna system with nonparallel beams. Both antennas lie on the *y* axis separated by a distance Δ. The angle θ_s is the angular offset from zenith in the *yz* plane, while ϕ_s is the offset in the *xz* plane.

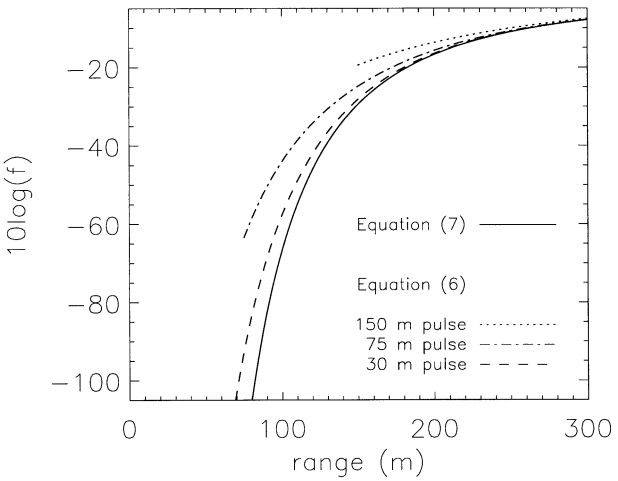

FIG. 2. Influence of transmit pulse length on baseline parallax correction for a dual-antenna radar system as a function of range with $\theta_o = 0.2°$ and $\Delta = 1$ m. Beyond 150 m the spread of values for $f(r)$ is negligible.

As Fig. 5 illustrates, $f(r)$ is sensitive to Δ at low altitudes. For example, at a height of 250 m, a 15-cm (or 15%) increase in Δ translates into a 4-dB decrease in $f(r)$. However, this sensitivity decreases significantly with height.

3. Measurement of parallax error

A parallax correction factor $[\hat{f}(r)]$ for the Penn State radar is estimated from the ratio of Penn State reflectivity measurements ($Z_{e,\text{dual}}$) to UMass reflectivity measurements ($Z_{e,\text{single}}$):

$$\left(\frac{Z_{e,\text{dual}}(r)}{Z_{e,\text{single}}(r)}\right) \approx \hat{f}(r)\delta\beta, \tag{10}$$

where $\delta\beta = \beta_{\text{dual}}/\beta_{\text{single}}$ is a range-independent calibration offset between the two radars and is not related to parallax. Although time dependence is not explicitly indicated, both $\hat{f}(r)$ and $\delta\beta$ are functions of time.

a. Low-altitude liquid clouds

As illustrated in Fig. 4, the shape of $f(r)$ at low altitudes is sensitive to the sign of the alignment error. Therefore, deep low-level liquid clouds, heavy fog, and precipitation are ideal hydrometeor targets for estimating $f(r)$, θ_s, and ϕ_s, as well as $\delta\beta$, for a dual-antenna radar system. Such a case of low-level liquid clouds and fog occurred on 11 April 1994 at the U.S. Department of Energy (DOE) Atmospheric Radiadion Measurement (ARM) Program Southern Great Plains (SGP) Cloud and Radiation Testbed (CART) site, when the Penn State and UMass CPRS radar systems were collocated for a cloud observation experiment. The CPRS detected no depolarization on 11 April; hence, we can assume there were few flying insects that could contaminate the cloud data (Sekelsky et al. 1998). Time-averaged vertically pointing radar reflectivity profiles are plotted in Fig. 6, showing that the CPRS Ka-band (33 GHz) and W-band (95 GHz) reflectivity measurements diverge with height. This difference between the two sets of profiles is caused

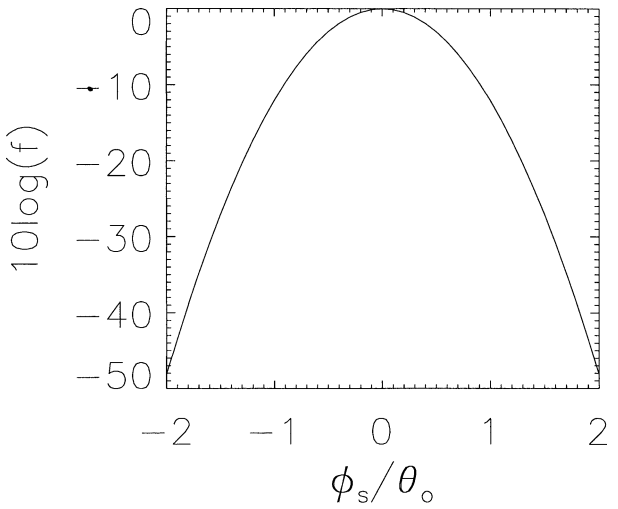

FIG. 3. Computation of dual-antenna parallax as a function of ϕ_s, which is normalized by the antenna half-power beamwidth (θ_o). The range is 900 m, $\theta_s = 0.0$, and $\Delta = 1$ m.

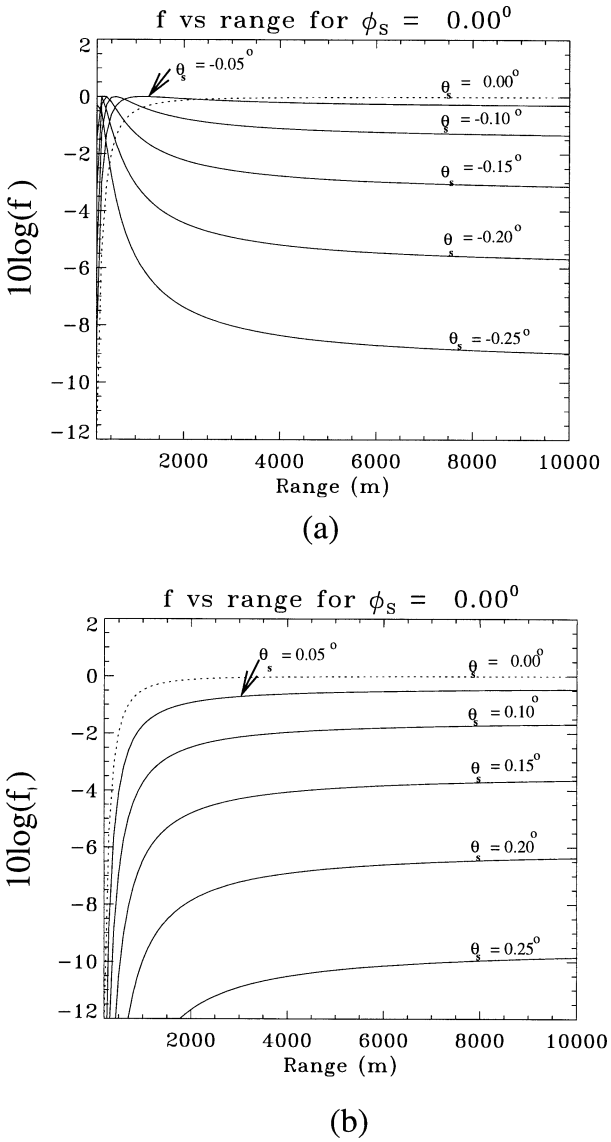

FIG. 4. Computation of dual-antenna parallax as a function of range (r) and θ_s. The values of θ_s are negative in (a) and positive in (b). The offset $\phi_s = 0.0$ and $\Delta = 1$ m.

by frequency-dependent attenuation (i.e., scattering and absorption) from cloud droplets and frequency-dependent absorption from water vapor and oxygen (Lhermitte 1990). Because of the possibility of scattering from relatively large drops (i.e., ''Mie scattering'') and differences in cloud and water vapor absorption, $f(r)$ is calculated using only W-band radar measurements.

Ratios Z_{dual}/Z_{single} of the reflectivity data illustrated in Fig. 6 are presented in Fig. 7, where the measured ratios of Z_{dual}/Z_{single} are averaged over 46 min and offset by -0.98 dB, which is the difference $\delta\beta$ in UMass and Penn State radar constants as determined from the offset of the measured from computed ratio curves. A least mean-squares fit of $f(r)$ in Eq. (7) to the measured data leads to angular offsets of $\theta_s = 0.052°$ and $\phi_s = \pm 0.068°$

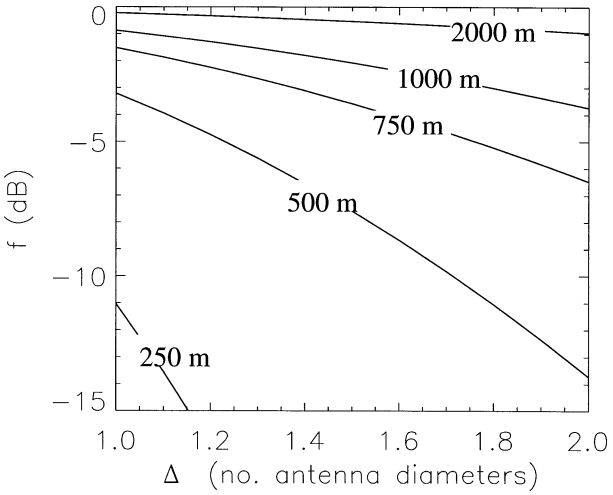

FIG. 5. Dependence of the baseline parallax correction [$f(r)$] on Δ at several altitudes. The antenna diameter (D) is 0.91 m and $\theta_o = 0.2°$.

for the Penn State radar transmit and receive antennas. Because parallax dependence on ϕ_s is symmetric (Fig. 3), it is not possible to resolve the sign ambiguity of ϕ_s.

The sensitivity to changes in θ_s and ϕ_s of the least root-mean-square difference fit of the model to the data is shown in Fig. 8 for the solutions $\theta_s = 0.052°$ and $\phi_s = +0.068°$. In the figure, contours of the root-mean-square difference between the measured parallax and model are plotted as a function of ϕ_s and θ_s. For example, the 5% contour indicates solutions with root-

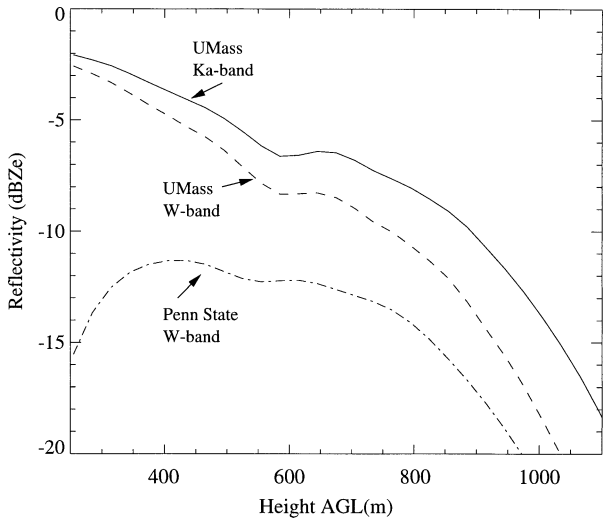

FIG. 6. UMass and Penn State radar reflectivity profiles averaged between 1900 and 1946 UTC. Divergence of UMass Ka-band and W-band data results from frequency dependence of gaseous and cloud extinction rates. Differences in UMass and Penn State W-band measurements are a result of parallax errors in the two-antenna Penn State system and a calibration difference between the two W-band systems.

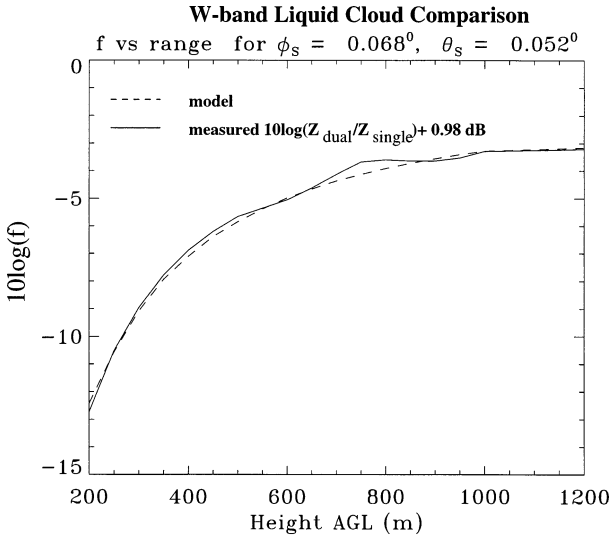

FIG. 7. Ratio of dual-antenna to single-antenna W-band reflectivity vs height. The solid curve is the ratio of W-band data plotted in Fig. 6, while the dashed curve is the best fit of $f(r)$ in Eq. (7) to the data. Note that the height range extent of the data is limited to 1.2 km, but the fit approaches 0 dB at larger ranges.

mean-square differences within 5% of the minimum value.

Summary histograms of the liquid cloud reflectivity data from 11 April 1994 for altitudes from 200 to 1200 m both before and after applying corrections for parallax, calibration offset, and attenuation are presented in Figs. 9 and 10. Reflectivity data plotted in Fig. 10 have been corrected for gaseous absorption and cloud extinction using models developed by Liebe (1985) and Liebe et al. (1989), together with sounding data from the ARM SGP CART site. Note that these corrections assume that the hydrometeors are small compared to the W-band radar wavelengths.

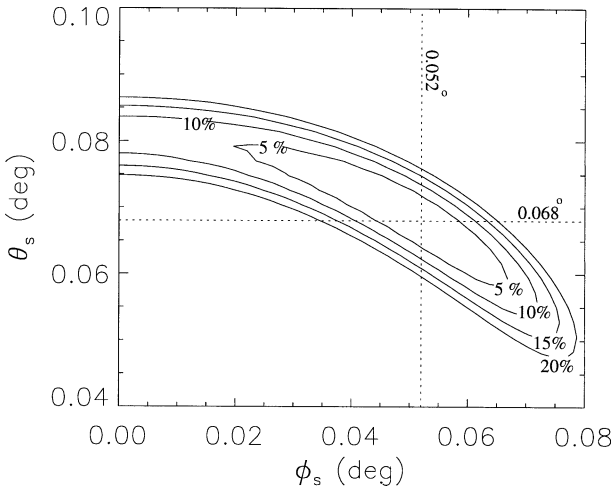

FIG. 8. Contour plot of root-mean-square differences between measured parallax data and model for values of θ_s and ϕ_s centered on a best-fit solution indicated by dashed lines.

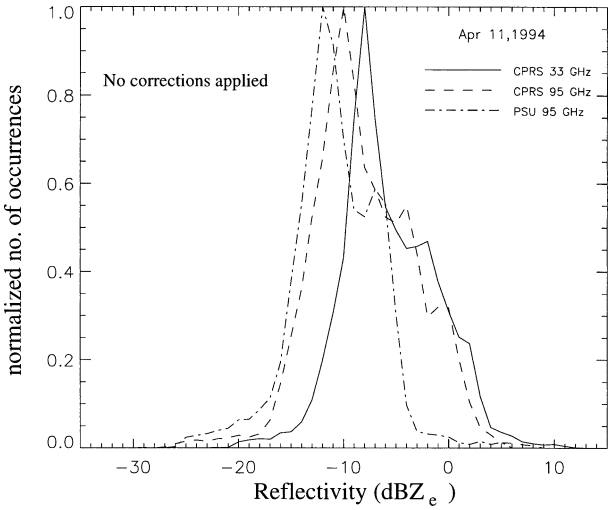

FIG. 9. Normalized histograms of uncorrected liquid water cloud reflectivity measurements for the three radar systems. The 70-min dataset spans altitudes from 200 to 1200 m, and the bin size is 1 dB.

b. *High-altitude cirrus clouds*

Unfortunately, the deep low-level liquid clouds and fog that we used to estimate $f(r)$ on 11 April 1994 were observed only once at the beginning of the ARM SGP CART site April 1994 cloud experiment. However, high-altitude cirrus clouds occurred after 11 April 1994, and we used reflectivity measurements from these clouds to monitor the product $f(r)\delta\beta$ throughout the remainder of the experiment. Because $f(r)$ is nearly independent of range at cirrus altitudes, it is not possible to separate variations of $f(r)$ from those of $\delta\beta$.

A detailed comparison of cirrus measurements for 15 April 1994 is shown in Figs. 11 and 12, which correspond to Figs. 8 and 9 for the liquid cloud case. At cirrus altitudes the baseline parallax correction for per-

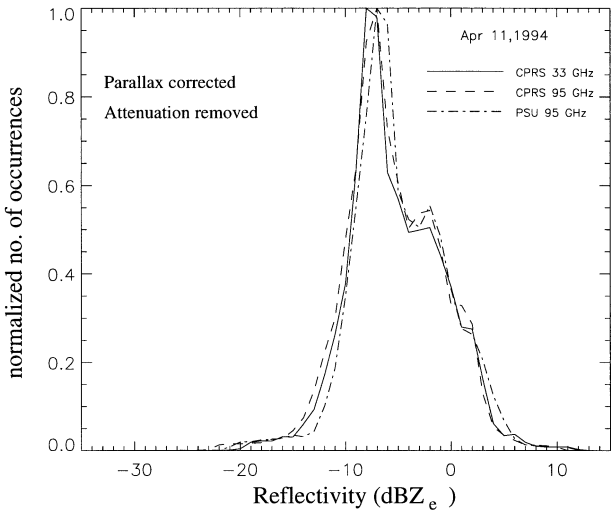

FIG. 10. Same data as in Fig. 9, but with corrections applied for attenuation, calibration offset, and dual-antenna parallax.

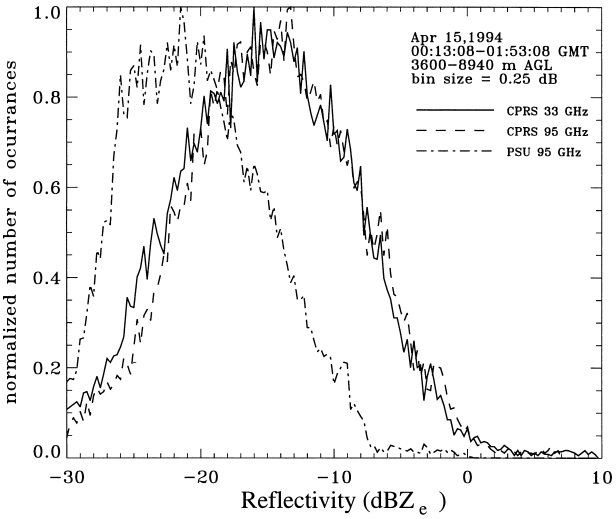

FIG. 11. Normalized histograms of uncorrected cirrus cloud reflectivity measurements for the three radar systems. The 140-min dataset spans altitudes from 3600 to 8940 m, and the bin size is 0.25 dB.

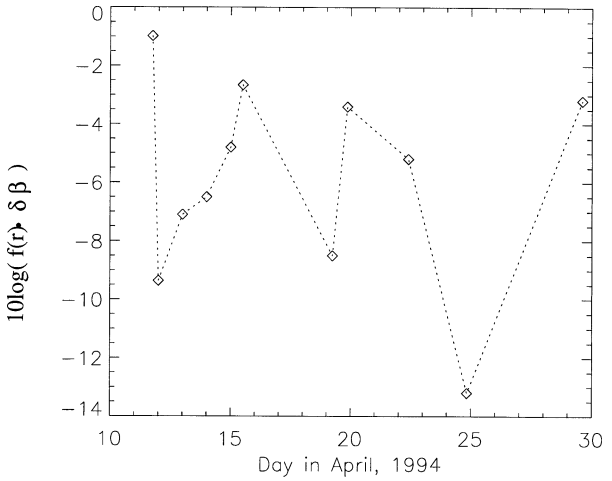

FIG. 13. Comparison of UMass single-antenna and Penn State dual-antenna radar system calibrations throughout the course of the ARM SGP CART site cloud experiment in April 1994. The first point is obtained from liquid clouds, as described in section 3a. Other points are obtained from cirrus cloud data, as described in section 3b. Note that a 0.2° error in the Penn State antenna alignment would produce the error observed on 25 April 1994.

fectly aligned antenna beams is negligible. However, the Penn State reflectivity values are approximately 6.3 dB lower than the UMass data for this day. For the liquid cloud case of 11 April, $f(r)\delta\beta$ is only -0.98 dB at these altitudes. Further comparisons of the product $f(r)\delta\beta$ from cirrus cloud reflectivities made during the experiment are plotted in Fig. 13.

Several possibilities may explain the large variations present in Fig. 13. The Penn State values are consistently lower than the UMass values, suggesting either a parallax problem, lowered values of β for the Penn State system, or elevated values of β for the UMass system. Because component performance problems will not increase β, but rather reduce it, we can conclude that either the antenna alignment or β, or both, for the Penn State radar was not stable over the course of the experimental period.

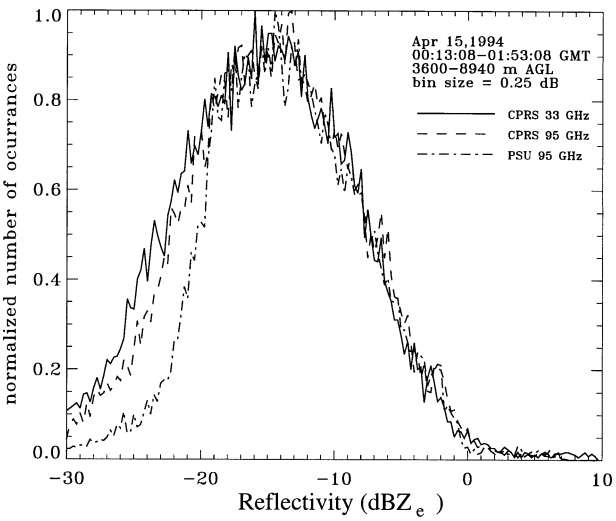

FIG. 12. Same data as in Fig. 11, but with corrections applied for attenuation and for the combined effects of calibration offset and dual-antenna parallax. Note that the left-hand edge of the Penn State histogram indicates a reduction in sensitivity of the Penn State radar vs the UMass radar.

4. Conclusions

The simulations and measurements presented show that dual-antenna atmospheric radars that use high-gain, narrow-beam antennas are likely to underestimate cloud reflectivity, unless extreme care is exercised to account for parallax and ensure stable antenna alignment. Dual-antenna radars, such as the Penn State system, typically have a spring-loaded mechanical adjustment to precisely set the angle of one antenna. The transmit and receive antennas of such a system are often aligned by observing high-altitude clouds and adjusting the pointing direction of one antenna so that the output of the receiver is maximized, but it is difficult to monitor the antenna alignment on a continuous basis, which may lead to undetected fluctuations in reflectivity data. To obtain accurate reflectivities from a dual-antenna system the range-dependent parallax correction factor [$f(r)$] must be determined by use of a model that includes accurate antenna pointing errors or by comparison of dual-antenna radar system reflectivities against simultaneous reflectivity measurements collected with a single-antenna radar.

Acknowledgments. The work presented was funded by the U.S. Department of Energy ARM Program under Grants DE-FG02-90ER61060 and DE-FG02-

90ER61071. The authors wish to thank the the SGP CART site personnel who supported the April 1994 cloud experiment, Greg Sadowy and John Galloway who supported the UMass radar deployment, and Xiquan Dong and David Babb who supported the Penn State radar deployment.

REFERENCES

Battan, L. J., 1973: *Radar Observation of the Atmosphere.* The University of Chicago Press, 161 pp.

Clothiaux, E. E., M. A. Miller, B. A. Albrecht, T. P. Ackerman, J. Verlinde, D. M. Babb, R. M. Peters, and W. J. Syrett, 1995: An evaluation of a 94-GHz radar for radar remote sensing of cloud properties. *J. Atmos. Oceanic Technol.,* **12,** 201–229.

Doviak, R. J., and D. S. Zrnić, 1984: *Doppler Radar and Weather Observations.* Academic Press, 458 pp.

Ferarro, P., 1992: A Ka-band stepped frequency scatterometer for the measurement of normalized radar cross sections. M.S. thesis, Electrical and Computer Engineering Dept. University of Massachusetts—Amherst.

Hobbs, P., N. T. Funk, R. R. Weiss, J. Locatelli, and K. Biswas, 1985: Evaluation of a 35 GHz radar for cloud physics research. *J. Atmos. Oceanic Technol.,* **2,** 35–48.

Klugmann, D., and R. Judaschke, 1995: A 94 GHz solid state FM-CW-Doppler radar profiler. *Conf. Proc. Second Topical Symp. on Combined Optical–Microwave Earth and Atmospheric Sensing,* Atlanta, GA, IEEE, 223–225. [Available for IEEE, 445 Hoes Ln., P. O. Box 1331, Piscataway, NJ 08855-1331.]

Lhermitte, R. M., 1987: A 94-GHz Doppler radar for cloud observations. *J. Atmos. Oceanic Technol.,* **4,** 36–48.

——, 1990: Attenuation and scattering of millimeter wavelength radiation by clouds and precipitation. *J. Atmos. Oceanic Technol.,* **7,** 464–479.

Liebe, H., 1985: An updated model for millimeter-wave propagation in moist air. *Radio Sci.,* **20,** 1069–1089.

——, T. Manabe, and G. A. Hufford, 1989: Millimeter wave attenuation and delay rates due to fog/cloud conditions. *IEEE Trans. Antennas Propag.,* **AP-37,** 1617–1623.

Mead, J. B., P. M. Langlois, P. S. Chang, and R. E. McIntosh, 1991: Polarimetric scattering from natural surfaces at 225 GHz. *IEEE Trans. Antennas Propag.,* **39,** 1405–1411.

Sekelsky, S. M., and R. E. McIntosh, 1996: Cloud observations with a polarimetric 33 GHz and 95 GHz radar. *Meteor. Atmos. Phys.,* **58,** 123–140.

——, and Coauthors, 1998: Comparison of millimeter-wave cloud radar measurements for the fall 1997 cloud IOP. *Proceeding of the Eighth Annual ARM Science Team Meeting,* N. Burleigh and D. Carrothers, Eds., U.S. Department of Energy.

Smith, P. L., 1986: On the sensitivity of weather radars. *J. Atmos. Oceanic Technol.,* **3,** 704–713.